

Thermal Performance Assessment for Laminar Forced Convection with Downstream Reformed-V and Reformed-Double-V Generators

¹Withada Jedsadaratanachai and ²Amnart Boonloi

¹Department of Mechanical Engineering, Faculty of Engineering, King Mongkut's Institute of Technology Ladkrabang, Bangkok 10520, Thailand

²Department of Mechanical Engineering Technology, College of Industrial Technology, King Mongkut's University of Technology North Bangkok, Bangkok 10800, Thailand

Article history

Received: 2014-04-04

Revised: 2014-10-30

Accepted: 2014-11-12

Corresponding Author:

Amnart Boonloi,
Department of Mechanical
Engineering Technology,
College of Industrial
Technology,
King Mongkut's University of
Technology North Bangkok,
Bangkok 10800, Thailand
Email: amp_g7@hotmail.com

Abstract: Thermal assessments for laminar flow in an isothermal wall square channel over downstream Reformed-V (RV) and Reformed-Double-V (RDV) generators inserted diagonally are presented numerically in three dimensional. The RV and RDV are designed to comfort for forming and installing in the heat exchanger channel. The effect of RV and RDV height is investigated in terms of blockage ratio, b/H , $BR = 0.05-0.30$ for Reynolds number based on the hydraulic diameter of the square channel, $Re = 100-1200$. The SIMPLE algorithm, finite volume method and the periodic condition are used in the current computational domain. The mathematical results show that the uses of RV and RDV provide higher heat transfer rate than the smooth square channel with no generators. The RV gives higher on both heat transfer rate and friction factor values than the RDV case for all BR and Re values. The maximum heat transfer rate and friction factor are found around 20.5 and 420 times over the smooth square channel, respectively, at $BR = 0.30$ for RV case. The optimum thermal enhancement factor, TEF, is found at $BR = 0.1$, $Re = 2000$ around 2.95 for RDV case.

Keywords: Forced Convection, Generators, Laminar Flow, Periodic Condition, Thermal Enhancement Factor

Introduction

The installation of the vortex generators is widely use in heat exchanger channel to improve the thermal performance. The V-shaped vortex generators are usually applied in the heat system, because it can create the impinging jet over the channel lead to the augmenting heat transfer rate and also increasing the thermal performance. However, the uses of the generators are remained the problems, such as; the installation method, the forming and the optimized generators shape, etc.

The investigations on the generators had been reported on both experimental and numerical. The numerical results can explain the phenomena of the flow structure that the way to develop the generators for occurring the maximum point of thermal enhancement factor. Therefore, this work is focused on the investigation with the numerical method. The Table 1 shows the numerical study of the vortex generators in heat transfer system.

Due to the forming and the installation of the generators in the heat exchanger channel are very important factors for industrial system, thus, the modified generators for comfortable to install had been investigated. The gaps which decreased the thermal performance and heat transfer rate were found when using the generators placed on the channel walls. The new designs of the generators which inserted diagonally in the square channel are interesting.

The major research objectives are as follows:

- To obtain numerical solutions for the heat exchanger channel with Reformed-V (RV) and Reformed-Double-V (RDV) vortex generators
- To explain the mechanism of heat transfer augmentation and flow visualization in square channel for the laminar forced convection regime
- To evaluate the thermal performance by using the RV and RDV generators

Table 1. The investigations of the vortex generators with numerical method

Authors	Studied cases	Nu/Nu ₀	f/f ₀	TEF
Jedsadaratanachai <i>et al.</i> (2011)	30° inclined baffle Inline, two opposite walls, square channel BR = 0.2 PR = 0.5-2.5 Re = 100-2000	1.00-9.20	1.00-21.50	3.78
Kwankaomeng and Promvonge (2010)	30° inclined baffle One side, square channel BR = 0.1-0.5 PR = 1.0-2.0 Re = 100-1000	1.00-9.23	1.09-45.31	3.10
Promvonge <i>et al.</i> (2010a)	30° inclined baffle Inline, two opposite walls, square channel BR = 0.1-0.3 PR = 1.0-2.0 Re = 100-2000	1.20-11.00	2.00-54.00	4.00
Promvonge and Kwankaomeng, (2010)	45° V-baffle Staggered, two opposite walls, AR = 2 channel BR = 0.05-0.3 PR = 1.0 Re = 100-1200	1.00-11.00	2.00-90.00	2.75
Promvonge <i>et al.</i> (2010b)	45° inclined baffle Inline-staggered, two opposite walls, square channel BR = 0.05-0.3 PR = 1.0 Re = 100-1000	1.50-8.50	2.00-70.00	2.60
Promvonge <i>et al.</i> (2012)	45° V-baffle Inline downstream, two opposite walls, square channel BR = 0.1-0.3 PR = 1.0-2.0 Re = 100-2000	1.00-21.00	1.10-225.00	3.80
Boonloi (2014)	20° V-baffle Inline downstream-upstream, two opposite walls, square channel BR = 0.1-0.3 PR = 1.0 Re = 100-2000	1.00-13.00	1.00-52.00	4.20
Boonloi and Jedsadaratanachai (2013)	30° V-baffle Downstream, one side, square channel BR = 0.1-0.5 PR = 1.0-2.0 Re = 100-1200	1.00-14.49	2.18-313.24	2.44
Jedsadaratanachai and Boonloi (2013)	45° Discrete-V-baffle Downstream, diagonally, square channel BR = 0.05-0.20 PR = 1.0-1.5 Re = 100-1200	1.40-8.10	2.50-36.00	2.50
Jedsadaratanachai and Boonloi (2014)	Single twisted tape y/W = 1.0-6.0 Re = 100-2000	1.00-10.00	3.00-44.00	3.51

Boundary Conditions and Assumptions

The boundary conditions and the assumptions of current mathematical models which referred from Promvonge *et al.* (2012) are as follows:

- The periodic boundaries are used for inlet and outlet of the domain
- The tested fluid is air with a temperature of 300 K (Pr = 0.7) and enter to the inlet with constant mass flow rate

- The inlet and outlet velocity profiles must be identical
- The physical properties of the air have been assumed to remain constant at average bulk temperature
- Impermeable boundary and no-slip wall conditions have been implemented over the square channel walls as well as the twisted tape
- The constant temperature of the channel walls is maintained at 310 K while the RV and RDV is assumed at adiabatic wall conditions
- Steady three-dimensional fluid flow and heat transfer
- The flow is laminar and incompressible
- Constant fluid properties
- Body forces and viscous dissipation are ignored.
- Negligible radiation heat transfer

Computational Domains, Grid Independent Test and Validation of the Smooth Channel

Figure 1 shows the square channel geometry with RV and RDV generators inserted diagonally. The

square channel height, H is set equal to 0.05 m, b is defined as the generators height, b/H is known as the blockage ratio. The spacing of the generators, P and P/H is identified as the pitch ratio of the generators. The distance from generators edge to tip is fixed at $0.5H$ on both RV and RDV. The case studies are presented as Table 2.

The characteristics of three grids; such as 80000, 120000 and 180000 cells, are adopted in the simulations for using the Grid Convergence Index (GCI) (Roache, 1998). The numerical results show similar trends and values on both Nu and f when using 120000 and 180000 cells. Therefore, the computational domain is set 120000 cells of the grid system for this work.

Table 2. Case studies

Case	BR	PR	Re
RV	0.05-0.30	1.00	100-1200
RDV	0.05-0.30	1.00	100-1200

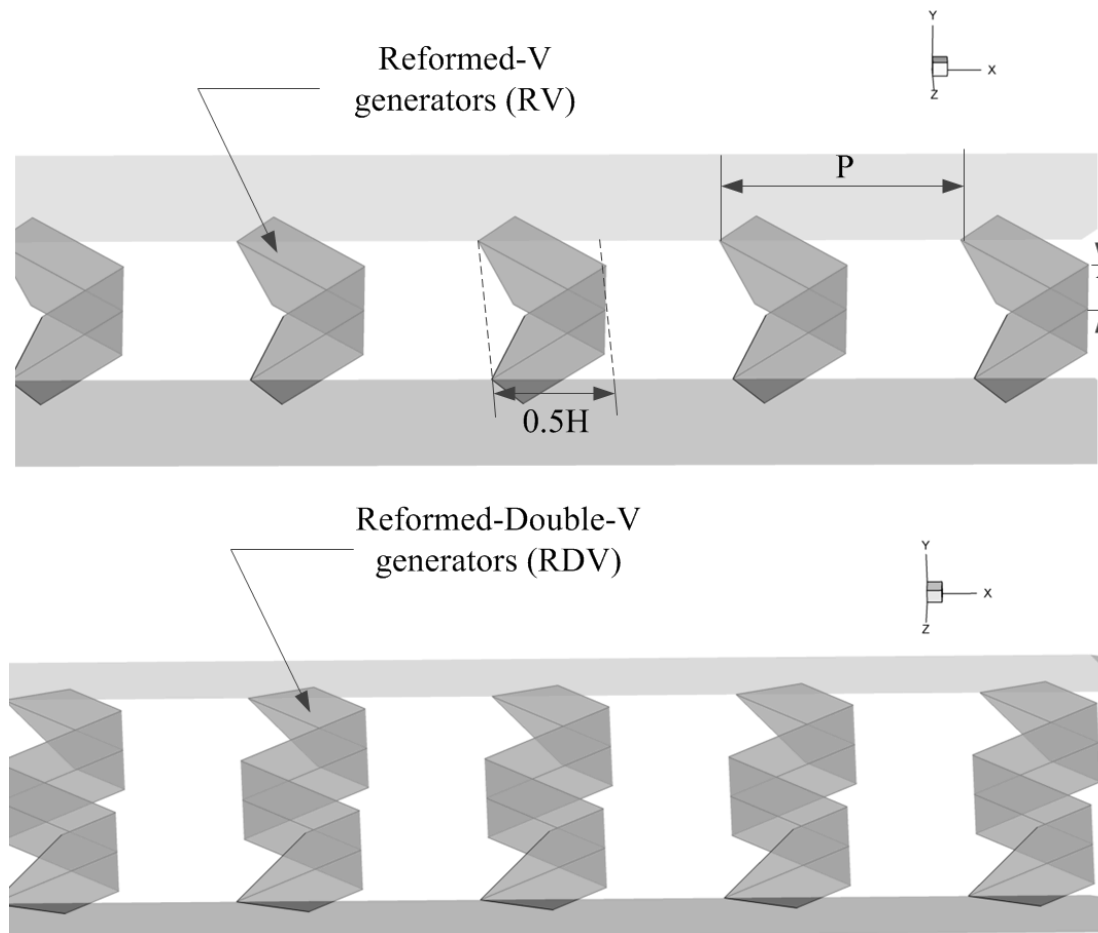


Fig. 1. Square channel geometry for RV and RDV generators

Table 3. Validation of smooth square channel

Re	Exact solution		Present prediction		Error (%)	
	Nu	f	Nu	f	Nu	f
100	2.98	0.57000	2.978	0.5710	0.0671	-0.1754
200	2.98	0.28500	2.975	0.2880	0.1678	-1.0526
300	2.98	0.19000	2.981	0.1910	-0.0336	-0.5263
400	2.98	0.14250	2.983	0.1430	-0.1007	0.0000
500	2.98	0.11400	2.983	0.1120	-0.1007	1.7544
600	2.98	0.09500	2.981	0.0950	-0.0336	0.0000
800	2.98	0.07125	2.988	0.0710	-0.2685	0.3509
1000	2.98	0.05700	2.988	0.0570	-0.2685	0.0000
1200	2.98	0.04750	2.988	0.0475	-0.2685	0.0000

The numerical results on both Nu and f are compared among the present prediction and the exact solution under similar operating conditions. The result is found to be in excellent agreement with exact solution values obtained from the open literature (Incropera and Dewitt, 2006) for both the Nu and f, less than ±1.75% deviation as shown in Table 3. The exact solutions of Nu and f for laminar flow over plain square channel are presented as Equation 1 and 2, respectively:

$$Nu_0 = 2.98 \tag{1}$$

$$f_0 = \frac{64}{Re} \tag{2}$$

Mathematical Foundation

The mathematical foundations for the current work are referred from Promvonge *et al.* (2012). The continuity equation, the momentum equation and the energy equation can be written as follows:

Continuity Equation 3:

$$\frac{\partial}{\partial x_i}(\rho u_i) = 0 \tag{3}$$

Momentum Equation 4:

$$\frac{\partial(\rho u_i u_j)}{\partial x_j} = -\frac{\partial p}{\partial x_i} + \frac{\partial}{\partial x_j} \left[\mu \left(\frac{\partial u_i}{\partial x_j} + \frac{\partial u_j}{\partial x_i} \right) \right] \tag{4}$$

Energy Equation 5:

$$\frac{\partial}{\partial x_i}(\rho u_i T) = \frac{\partial}{\partial x_j} \left(\Gamma \frac{\partial T}{\partial x_j} \right) \tag{5}$$

where, Γ is the thermal diffusivity and is given by:

$$\Gamma = \frac{\mu}{Pr} \tag{6}$$

Except from the energy equation discretized by the QUICK scheme, the governing equations were discretized by the Second Order Upwind (SOU) scheme, decoupling with the SIMPLE algorithm and solved by using a finite volume approach (Patankar, 1980). The solutions are measured to be converged when the normalized residual values were less than 10^{-5} for all variables but less than 10^{-9} only for the energy equation.

The parameters; Reynolds number, friction factor, Nusselt number, average Nusselt number and thermal enhancement factor are presented as Equation 7 to 11, respectively:

$$Re = \rho \bar{u} D / \mu \tag{7}$$

$$f = \frac{(\Delta p / P) D}{\frac{1}{2} \rho \bar{u}^2} \tag{8}$$

$$Nu_x = \frac{h_x D}{k} \tag{9}$$

$$Nu = \frac{1}{A} \int Nu_x \partial A \tag{10}$$

The Thermal Enhancement Factor (TEF) is defined as the ratio of the heat transfer coefficient of an augmented surface, h to that of a smooth surface, h_0 , at an equal pumping power and given by:

$$TEF = \frac{h}{h_0} \Big|_{pp} = \frac{Nu}{Nu_0} \Big|_{pp} = (Nu/Nu_0) / (f/f_0)^{1/3} \tag{11}$$

where, Nu_0 and f_0 stand for Nusselt number and friction factor for the plain square channel, respectively.

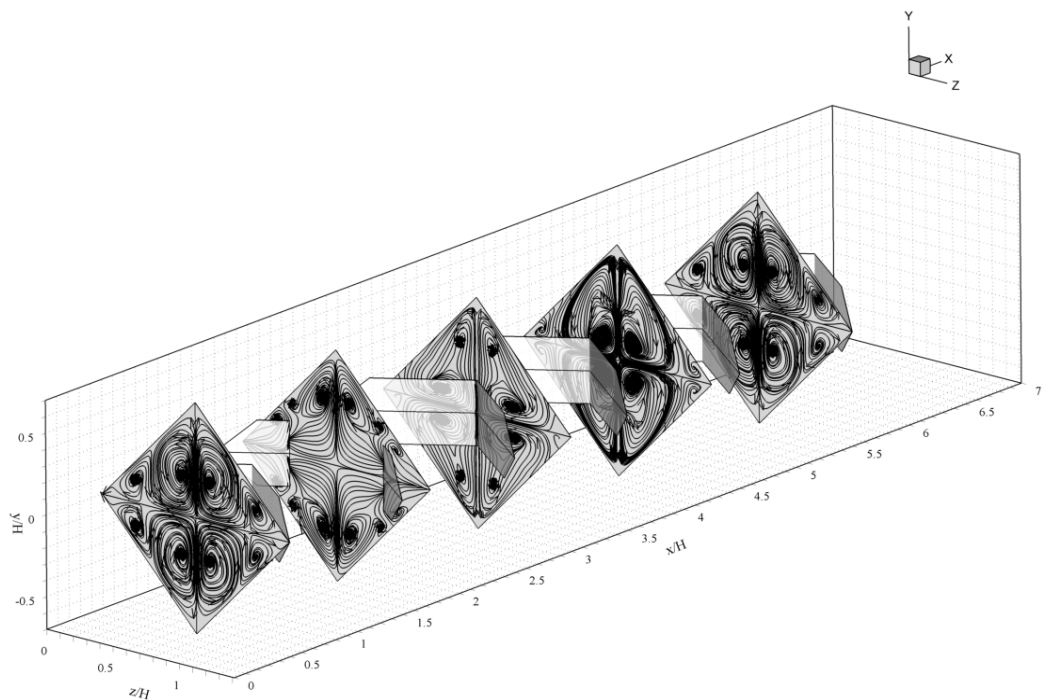
Results and Discussion

Flow Configurations and Heat Transfer Characteristics

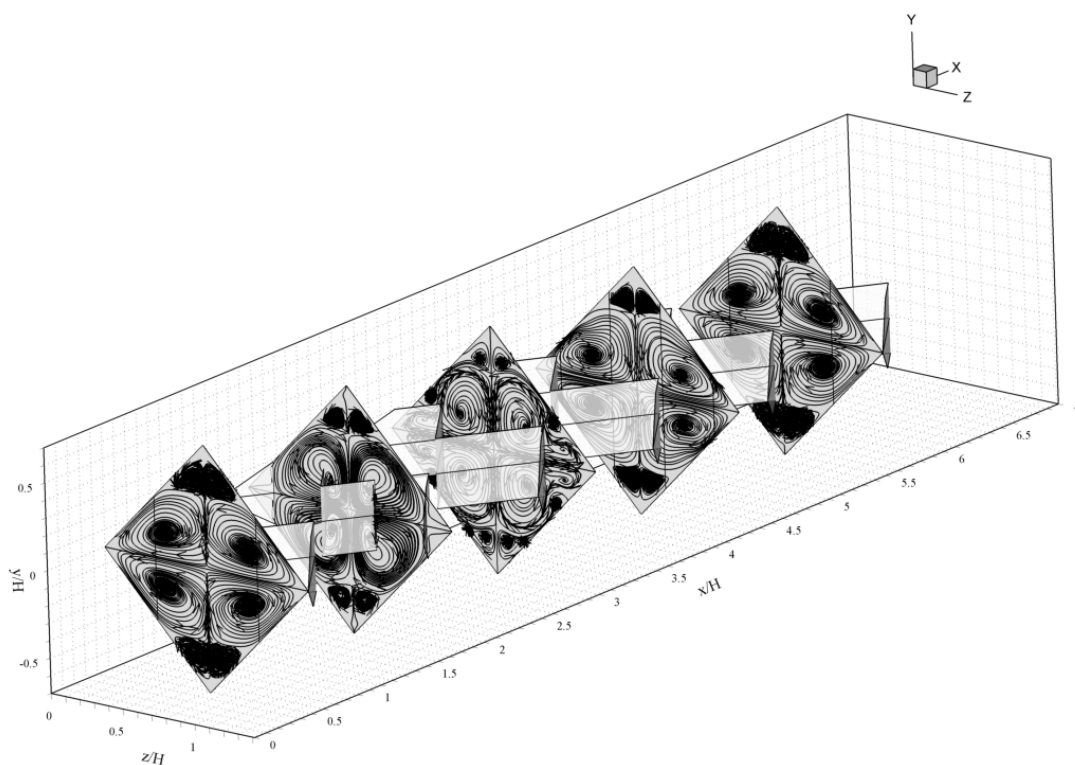
The flow configurations are reported in term of streamlines in transverse planes as Fig. 2, while the

heat transfer characteristics are presented in forms of contour temperature in transverse planes and

contours of local Nusselt number as Fig. 3 and 4, respectively.

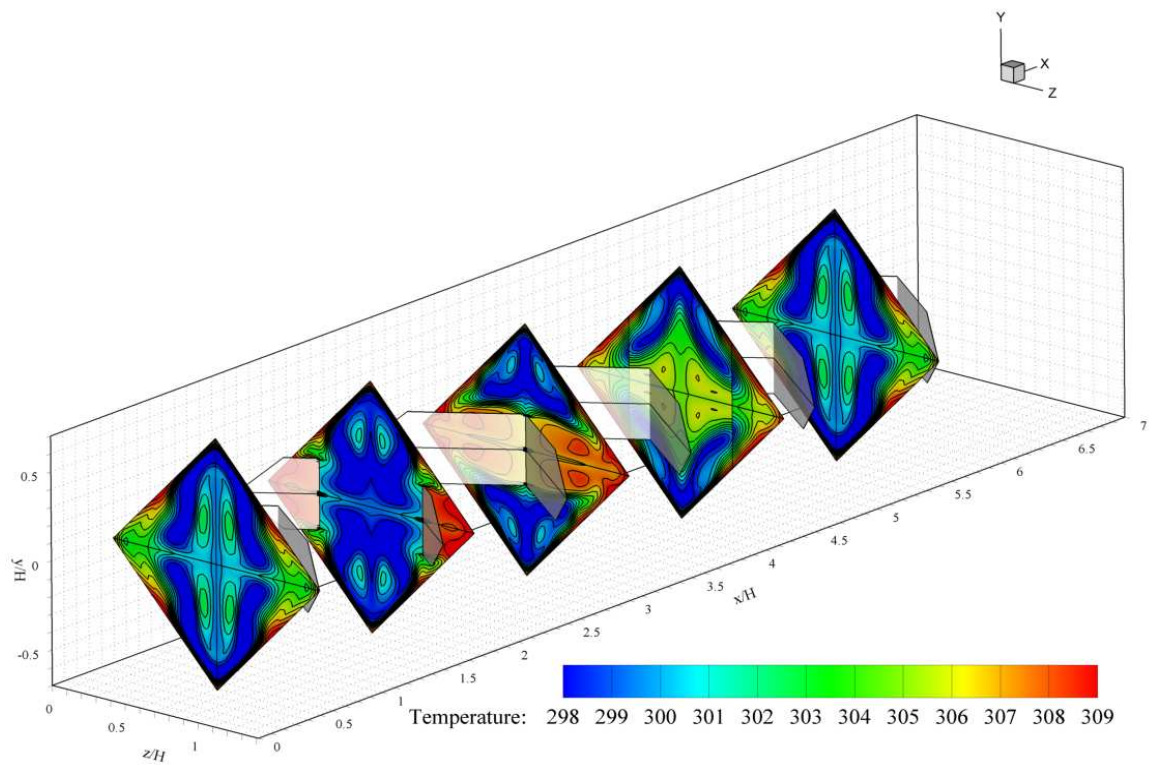


(a)

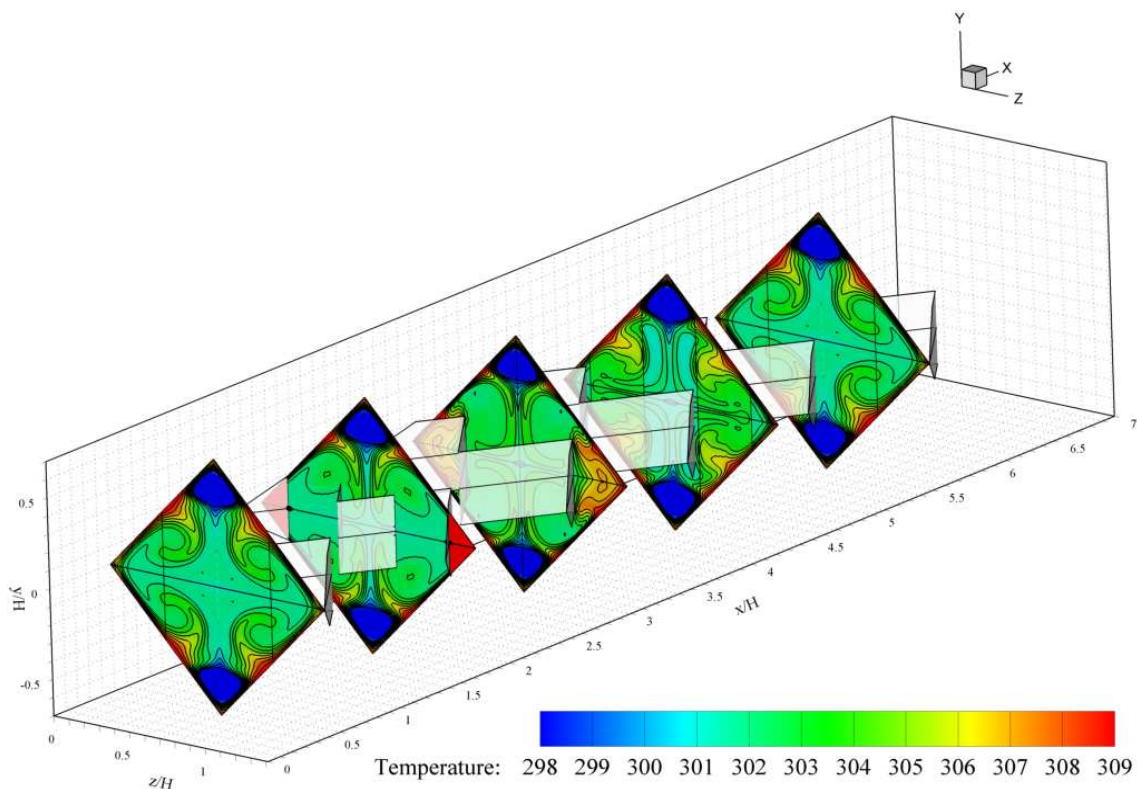


(b)

Fig. 2. Streamlines in transverse planes for (a) RV and (b) RDV at $Re = 1200$ and $BR = 0.20$



(a)



(b)

Fig. 3. Temperature contours in transverse planes for (a) RV and (b) RDV at $Re = 1200$ and $BR = 0.20$

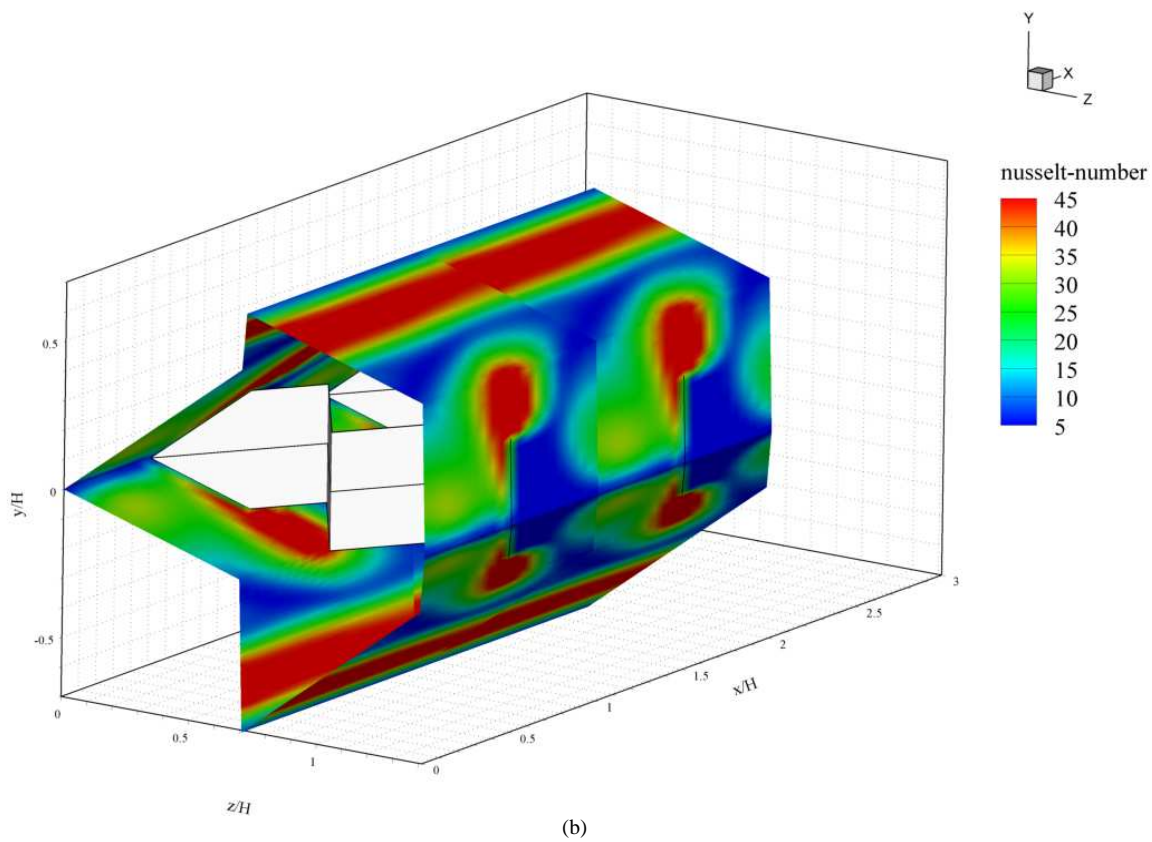
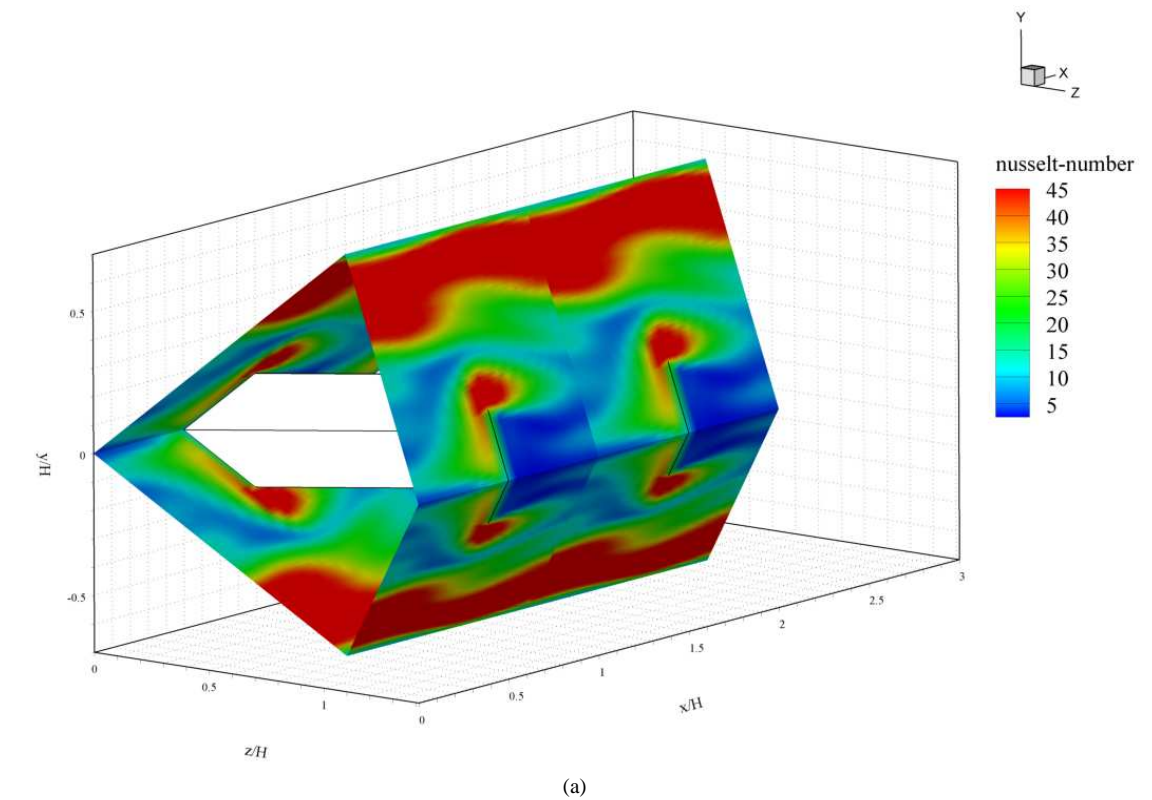


Fig. 4. Nu_x contours for (a) RV and (b) RDV at $Re = 1200$ and $BR = 0.20$

Figure 2a and b present the streamlines in transverse planes for RV and RDV, respectively, at $Re = 800$ and $BR = 0.2$. There are found that the inserted RV and RDV can change the flow field in comparison with the smooth square channel. The counter-rotating flow with common-flow-down is appearing for RV case when considering at the lower part of the main vortex. The similar flow structure with different rotating direction is found in case RDV. The vortex flows for RV are seen to be full filled of the transverse planes while the RDV provide a smaller size, but give the small vortices on both the upper and lower corner of the tested channel.

Figure 3a and b show the heat transfer behavior in the form of temperature in transverse planes for RV and RDV, respectively. As seen, on both the RV and RDV help to mixing the fluid flow between core and near the wall regimes. The RV case performs better mixing of the fluid flow than the RDV case.

Figure 4a and b display the Nu_x contours on the square channel walls for RV and RDV, respectively, at $BR = 0.2$ and $Re = 800$. The uses of RV and RDV

perform higher heat transfer rate than the smooth square channel. The peak regimes are found similarly. It is noted that the regimes where produce the lower heat transfer rate are found in case RDV, considering the blue contours over the channel walls.

Performance Assessment

The performance evaluations are presented for heat transfer rate, pressure loss and thermal performance in forms of Nusselt number ratio, Nu/Nu_0 , friction factor ratio, f/f_0 and thermal enhancement factor, TEF, respectively. Figure 5a and b present the Nu/Nu_0 versus Reynolds number and Nu/Nu_0 versus BR, respectively, for RV and RDV. In general, the increasing Reynolds number and BR result in the increasing heat transfer rate for all cases. At $BR = 0.30$, the RV performs higher heat transfer rate than the RDV around 2 times. For $0.05 \leq BR \leq 0.15$, the RDV provides higher heat transfer rate than the RV case but the reverse trends present when $BR > 0.15$.

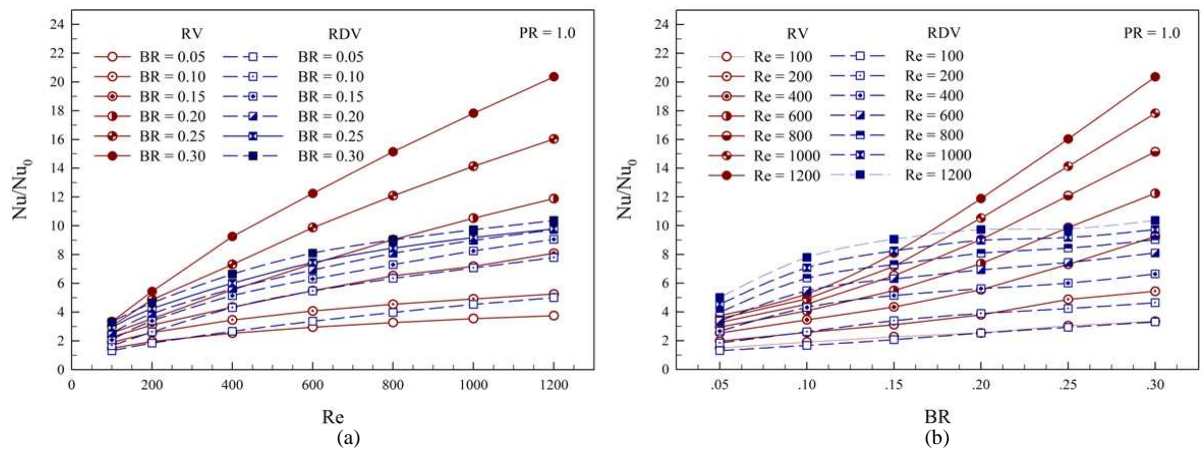


Fig. 5. (a) The variation of Nu/Nu_0 with Reynolds number and (b) The variation of Nu/Nu_0 with BRs

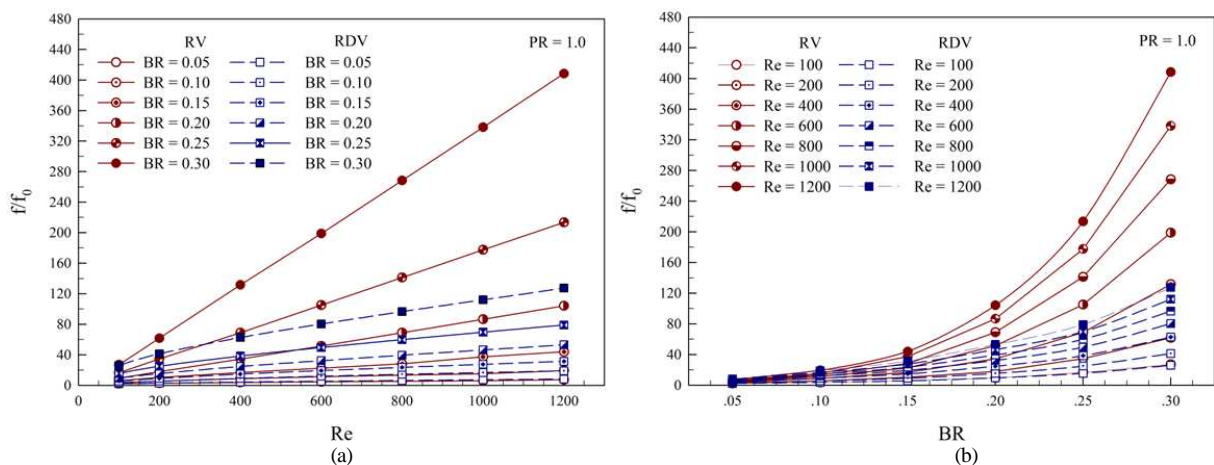


Fig. 6. (a) The variation of f/f_0 with Reynolds number and (b) The variation of f/f_0 with BRs

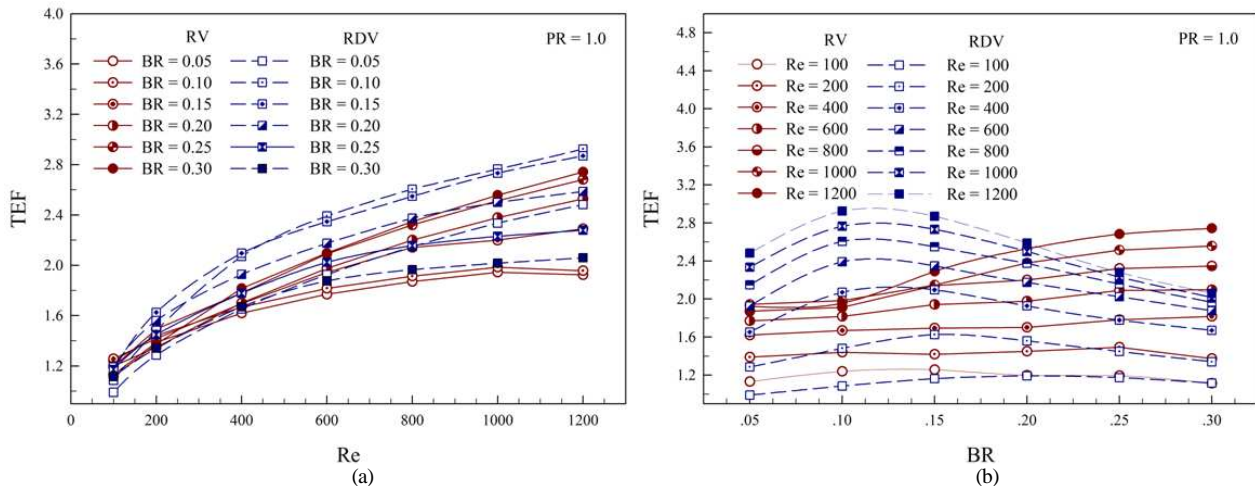


Fig. 7. (a) The variation of TEF with Reynolds number and (b) The variation of TEF with BRs

The uses of RV and RDV show the heat transfer rate around 1-20.5 and 1-10.5 times over the smooth square channel, respectively. Figure 6a and b show the f/f_0 with Re and the f/f_0 with BR, respectively, for RV and RDV cases. The rising Reynolds number and the blockage ratios effect for the increasing friction factor values, especially, at $BR > 0.2$ for RV case. The friction factors are around 1-120 and 1-430 for RV and RDV, respectively. The thermal enhancement factors are presented in Fig. 7a and b, respectively, for RV and RDV. The uses on both cases give the TEF around 1-2.6 and 1-2.95 for RV and RDV, respectively. The optimum points are found at $BR = 0.10$, $Re = 1200$ for RDV case.

Conclusion

The thermal performance assessments for laminar forced convection in a square channel with RV and RDV generators are presented numerically in a three dimensional. The effects of BRs on flow configurations and heat transfer characteristics of Reynolds number, $Re = 100-1200$ are investigated. The summarizations are as follows:

- The rising Reynolds number and BR provide increasing heat transfer rate and friction factors in all cases
- The augmenting heat transfer rate is around 1-20.5 and 1-10.5 for RV and RDV, respectively, while the friction factor has seemed to be around 1-430 and 1-120
- The thermal enhancement factor is around 1-2.6 and 1-2.95 for RV and RDV, respectively. The optimum TEF is found at $BR = 0.10$ for RDV case at the highest Reynolds number, $Re = 1200$

Acknowledgement

The authors would like to thank King Mongkut's Institute of Technology Ladkrabang (KMUTL) research fund for financial supports.

Author's Contributions

All authors equally contributed in this work.

Ethics

This article is original and contains unpublished material. The corresponding author confirms that all of the other authors have read and approved the manuscript and no ethical issues involved.

References

Boonloi, A. and W. Jedsadaratanachai, 2013. 3D Numerical study on laminar forced convection in V-baffled square channel. *Am. J. Appl. Sci.*, 10: 1287-1297. DOI: 10.3844/ajassp.2013.1287.1297

Boonloi, A., 2014. Effect of flow attack angle of V-ribs vortex generators in a square duct on flow structure, heat transfer and performance improvement. *Modell. Simulat. Eng.*, 2014: 985612-985622. DOI: 10.1155/2014/985612

Incropera, F.P. and P.D. Dewitt, 2006, *Introduction to Heat Transfer*. 5rd Edn., John Wiley and Sons, Hoboken, NJ., ISBN-10: 0471457272, pp: 912.

Jedsadaratanachai, W. and A. Boonloi, 2013. Energy performance improvement, flow behavior and heat transfer investigation in a circular tube with V-downstream discrete baffles. *J. Math. Stat.*, 9: 339-348. DOI: 10.3844/jmssp.2013.339.348

- Jedsadaratanachai, W. and A. Boonloi, 2014. Effect of twisted ratio on flow structure, heat transfer and thermal improvement in a circular tube with single twisted tape. *J. Math. Stat.*, 10: 80-91.
DOI: 10.3844/jmssp.2014.80.91
- Jedsadaratanachai, W., S., Suwannapan and P. Promvong, 2011. Numerical study of laminar heat transfer in baffled square channel with various pitches. *Energy Procedia*, 9: 630-642.
DOI: 10.1016/j.egypro.2011.09.073
- Kwankaomeng, S. and P. Promvong, 2010. Numerical prediction on laminar heat transfer in square duct with 30° angled baffle on one wall. *Int. Commun. Heat Mass Transfer*, 37: 857-866.
DOI: 10.1016/j.icheatmasstransfer.2010.05.005
- Patankar, S.V., 1980, *Numerical Heat Transfer and Fluid Flow*. 1st Edn., McGraw-Hill, New York, ISBN-10: 0070487405, pp: 197.
- Promvong, P. and S. Kwankaomeng, 2010. Periodic laminar flow and heat transfer in a channel with 45° staggered V-baffles. *Int. Commun. Heat Mass Transfer*, 37: 841-849.
DOI: 10.1016/j.icheatmasstransfer.2010.04.002
- Promvong, P., S. Sripattanapipat and S. Kwankaomeng, 2010b. Laminar periodic flow and heat transfer in square channel with 45° inline baffles on two opposite walls. *Int. J. Therm. Sciences*, 49: 963-975.
DOI: 10.1016/j.ijthermalsci.2010.01.005
- Promvong, P., W. Jedsadaratanachai and S. Kwankaomeng, 2010a. Numerical study of laminar flow and heat transfer in square channel with 30° inline angled baffle turbulators. *Appl. Therm. Eng.*, 30: 1292-1303.
DOI: 10.1016/j.applthermaleng.2010.02.014
- Promvong, P., W. Jedsadaratanachai, S. Kwankaomeng and C. Thianpong, 2012. 3D simulation of laminar flow and heat transfer in V-baffled square channel. *Int. Commun. Heat Mass Transfer*, 39: 85-93.
DOI: 10.1016/j.icheatmasstransfer.2011.09.004
- Roache, P.J., 1998. *Verification and Validation in Computational Science and Engineering*. 1st Edn., Hermosa Publishers, Albuquerque, NM, ISBN-10: 0913478083, pp: 464.